Crystal Structure of Interleukin-21 Receptor (IL-21R) Bound to IL-21 Reveals That Sugar Chain Interacting with WSXWS Motif Is Integral Part of IL-21R*[S]

Ole J. Hamming[‡], Lishan Kang[§], Anders Svensson[¶], Jesper L. Karlsen[‡], Henrik Rahbek-Nielsen[¶], Søren R. Paludan[||], Siv A. Hjorth[¶], Kent Bondensgaard[¶], and Rune Hartmann[‡1]

From the Departments of [‡]Molecular Biology and Genetics and [||]Biomedicine, Aarhus University, DK-8000 Aarhus C, Denmark, [§]Novo Nordisk China R&D, Beijing 102206, China, and the [¶]Biopharmaceuticals Research Unit, Novo Nordisk A/S, DK-2760 Maaloev, Denmark

Background: The class I cytokine IL-21 exerts pleiotropic effects on innate and adaptive immunity.
Results: We obtained the crystal structure of the partially glycosylated IL-21 receptor (IL-21R) bound to IL-21.
Conclusion: A sugar chain is an integral part of IL-21R.
Significance: This structure offers an insight into the putative role of the class I cytokine receptor signature motif.

IL-21 is a class I cytokine that exerts pleiotropic effects on both innate and adaptive immune responses. It signals through a heterodimeric receptor complex consisting of the IL-21 receptor (IL-21R) and the common γ-chain. A hallmark of the class I cytokine receptors is the class I cytokine receptor signature motif (WSXWS). The exact role of this motif has not been determined yet; however, it has been implicated in diverse functions, including ligand binding, receptor internalization, proper folding, and export, as well as signal transduction. Furthermore, the WXXW motif is known to be a consensus sequence for C-mannosylation. Here, we present the crystal structure of IL-21 bound to IL-21R and reveal that the WSXWS motif of IL-21R is C-mannosylated at the first tryptophan. We furthermore demonstrate that a sugar chain bridges the two fibronectin domains that constitute the extracellular domain of IL-21R and anchors at the WSXWS motif through an extensive hydrogen bonding network, including mannosylation. The glycan thus transforms the V-shaped receptor into an A-frame. This finding offers a novel structural explanation of the role of the class I cytokine signature motif.

IL-21 is a class I cytokine with a four-helix bundle structure arranged in an up-up-down-down topology typical for the class I cytokines (1). It exerts pleiotropic effects on both innate and adaptive immune responses. IL-21 is secreted by activated CD4$^+$ T cells, in particular T$_H$17 and T follicular helper cells, as well as natural killer cells (2). Not only do both T$_H$17 and T follicular helper cells produce IL-21, but this cytokine also plays

an important role in promoting the development of T$_H$17 and T follicular helper cells by a feed-forward mechanism (3–8). Furthermore, IL-21 cooperates with other cytokines to increase the cytotoxicity of CD8$^+$ T cells and promotes proliferation of CD8$^+$ cells in the presence of antigens (9). IL-21 also influences antibody production by B cells (10). Recent studies demonstrated that IL-21 produced by CD4$^+$ cells is critical for the ability of CD8$^+$ T cells to control viral infection (11–13). The ability of IL-21 to augment immunity has spurred substantial interest in the therapeutic use of IL-21, and it is currently being evaluated in a number of clinical trials against, for example, metastatic melanoma and renal cancer (14).

IL-21 signals through a heterodimeric receptor complex consisting of the private chain IL-21 receptor (IL-21R)[2] and the common γ-chain (γC), the latter being shared by IL-2, IL-4, IL-7, IL-9, and IL-15 (15). Upon binding of IL-21 to the receptor complex and subsequent receptor activation, signaling occurs through the Jak-STAT signaling pathway (16). The IL-21R chain binds IL-21 with high affinity and provides the majority of the binding energy (17). However, interaction with γC is required for signaling (16), and IL-21 mutants that bind IL-21R but fail to interact properly with γC act as potent antagonists of IL-21 signaling (1).

Several structures of γC class cytokines bound to one or more of their receptor chains have been solved (18–22). The receptors generally adopt very similar structures, with two type III fibronectin domains separated by a short linker. Each receptor chain adopts a V-shape, with the ligand binding at the tip of the V. The fibronectin domains each contain seven β-strands forming a sandwich-like structure. Binding of the ligand to the receptor engages residues present within the loops of both fibronectin domains.

Receptors of the γC cytokines are known to be universally N-glycosylated (20). This glycosylation is not required, however, for formation of the ligand-receptor complexes, as structures using receptors purified from *Escherichia coli* have been

---

solved (20, 22). Still, the binding affinity between IL-7 and IL-7R has been demonstrated to be increased when IL-7R is glycosylated (20). Whether this is also the case for other members of the family remains to be determined.

The class I cytokine receptor family is characterized by the presence of the so-called class I cytokine receptor signature motif in the second fibronectin domain (24). The consensus sequence of the motif is WS*X*WS (present in 28 of 36 investigated sequences (25)). Several possible functional roles of the WS*X*WS sequence have been suggested, including involvement in ligand binding, receptor internalization, proper folding, export, and signal transduction (25–28). Although numerous studies have addressed the functional role of this highly conserved receptor motif, no clear picture has emerged. However, the first structures of class I cytokine receptors have clearly demonstrated that the motif is not directly involved in ligand binding (18–22, 29). Furthermore, despite the highly conserved nature of this motif, considerable sequence diversity is tolerated as demonstrated by several mutagenesis studies (25–27). The most extreme example is the human growth hormone receptor, in which the motif has the sequence YTEFS rather than WS*X*WS (30).

Interestingly, W*XX*W is known to be a consensus sequence for *C*-mannosylation, where a mannose is attached to the first tryptophan (31), and this kind of modification has indeed been found in the WS*X*WS motif of the class I cytokine receptors IL-12B and EPOR (32, 33). The structures of class I cytokine receptors solved so far have not included this modification, possibly because the proteins have been produced in either insect cells or *E. coli*, where this modification is not made. The mechanism and potential function of this modification are currently unknown.

EXPERIMENTAL PROCEDURES

Protein Expression and Purification—IL-21 was expressed and purified from *E. coli* as described previously (34). The extracellular domain (ECD) of IL-21R was expressed in HEK293 cells and purified as described (1).

Complex Formation—The complex of IL-21 and IL-21R was formed by mixing IL-21 and IL-21R at room temperature at a ratio of 1.5:1. Elevated levels of IL-21 were used, as IL-21 is most readily available. Furthermore, as IL-21 (15–16 kDa) is much smaller than IL-21R (28 kDa), it is more easily separated from the complex (43 kDa) after gel filtration. The complex was loaded onto a HiLoad 16/60 Superdex 75 column (GE Healthcare) and eluted with PBS (10 mM phosphate and 150 mM NaCl, pH 7.4). The fractions containing the complex were concentrated to 5 mg/ml using an Amicon Ultra-4 centrifugal filter device with a 10,000 M_r cutoff.

Crystallization—All crystals were grown at 18 °C as sitting drops with a reservoir solution containing 500 μl of 1.8–1.9 M diammonium sulfate and 0.1 M sodium acetate at pH 5.5. 1 μl of reservoir solution and 1 μl of protein solution were mixed in the pedestal. Large single crystals appeared after 10–14 days. These were flash-frozen using a cryosolution containing 3.0 M diammonium sulfate and 0.1 M sodium acetate at pH 5.5. Tantalum bromide derivatives were obtained by adding 0.1 μl of a 2 mM $Ta_6Br_{12}^{2+}$ solution. This was left for 2 h, at which point the

crystals had turned green, indicating uptake of $Ta_6Br_{12}^{2+}$. The crystals were flash-cooled using a cryosolution containing 3.0 M diammonium sulfate and 0.1 M sodium acetate at pH 5.5. Crystals of selenomethionine IL-21 in complex with IL-21R were produced in the same way as for the wild type.

Data Collection and Processing—All data were collected at the Swiss Light Source at the PXIII (X06DA) beamline at 77 K (196 °C). For the native data set, 180 frames were collected with an oscillation of 1° at a wavelength of 0.98 Å. For the selenomethionine IL-21 data set, 720 frames were collected with an oscillation of 1° at a wavelength of 0.98 Å, and for the tantalum bromide data set, 1080 frames were collected with an oscillation of 1° at a wavelength of 0.98 Å. All data sets were indexed and scaled using XDS (35). All data sets belong to space group $P2_12_12_1$, with cell dimensions of $83 \times 152 \times 365$ Å. See Table 1 for details.

Phasing—Sites for the $Ta_6Br_{12}^{2+}$ derivative were found using SHELXE and SHELXD (36), and phases were calculated using Phenix (37). Phasing was done at 6 Å, where Ta_6Br_2 scattering approximates a single heavy atom. 25 initial sites were found in SHELXE using both anomalous and isomorphous data. Of these, 16 highest scoring sites were chosen for refinement in Phenix. Upon manual inspection, 15 of the initial 16 sites were selected for phasing. The phases from the $Ta_6Br_{12}^{2+}$ data set were used to find sites in the selenomethionine IL-21 data set using anomalous difference Fourier maps. This gave 50 initial hits. Manual inspection of these sites revealed that 20 were positioned as three sites with 8-fold symmetry, with four sites missing. Human IL-21 contains four methionines, but from the available NMR structure (34), we knew that two of these (Met[10] and Met[118]) are close in the structure. This makes it likely that they would be seen as a single site at 6 Å. Initial phases were calculated from the $Ta_6Br_{12}^{2+}$ derivative, followed by density modification in Resolve. Using the selenomethionine IL-21 sites, eight copies of the known NMR structure of IL-21 were placed in the map. From this, initial NCS operators were calculated, and density modification was repeated using this 8-fold NCS. A polyalanine model of IL-2RB was created and divided into its two constituent fibronectin domains. These were placed in the regions of the map containing density for IL-21R. Using Resolve (38), one NCS group with eight operators was made for IL-21, as well as for each of the two fibronectin domains of IL-2RB. Upon refinement of the NCS operators, a final round of density modification and phase extension to 3.5 Å was performed in Resolve. The resulting map was of excellent quality at the resolution, and the IL-21R structure was built *de novo* by repeated cycles of building and refinement in Coot (39) and Phenix, respectively. The final model contains eight molecules of IL-21R and IL-21, forming the IL-21R·IL-21 complex refined to a resolution of 2.8 Å. Evaluation of the Ramachandran plot in Coot showed 94.25% and 5.75% in preferred and allowed regions, respectively.

RESULTS

Overall Structure—We have determined the structure of IL-21 in complex with the ECD of its private receptor chain IL-21R at a resolution of 2.8 Å (Fig. 1*A* and Table 1). The unit cell contains eight IL-21R·IL-21 complexes. The core structures
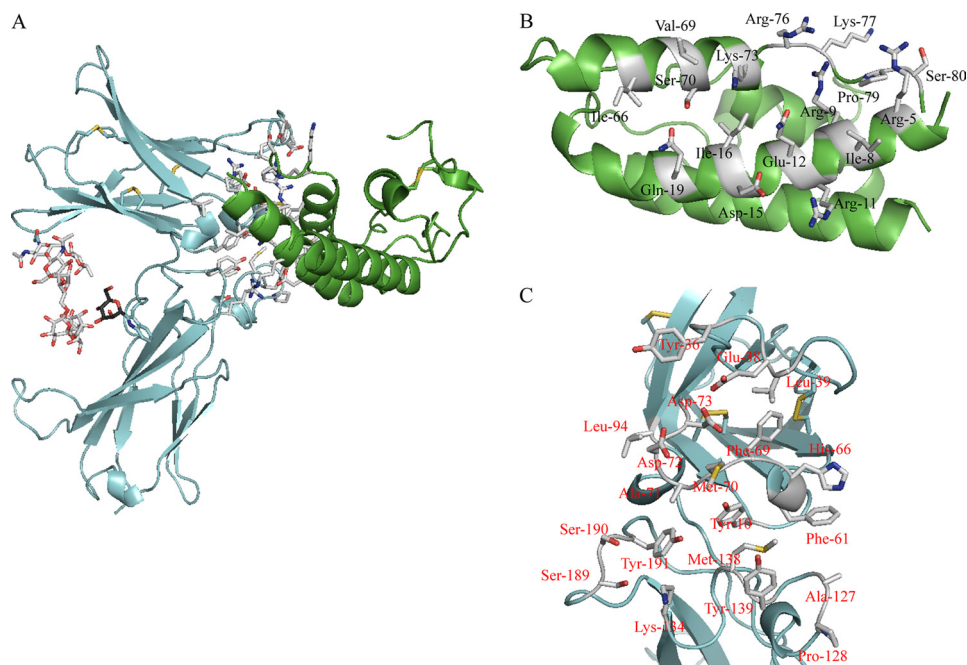
FIGURE 1. **Residues in IL-21 and IL-21R involved in binding.** *A*, structure of the IL-21R·IL-21 complex, with residues involved in the interaction between IL-21 and IL-21R shown in *white*. IL-21 is shown in *green*, and IL-21R is shown in *cyan*. The sugar chain originating from Asn[54] is shown in *white*, and the mannose on Trp[195] is shown in *black*. Distance criteria for contact assignments are ≤4.5 for van der Waals contacts and ≤3.5 for hydrogen bonds and polar interactions. *B*, residues in IL-21 involved in binding IL-21R. *C*, residues in IL-21R involved in binding IL-21.

TABLE 1

Data collection and refinement statistics for the IL-21R·IL-21 complex

SLS, Swiss Light Source; FOM, figure of merit; r.m.s.d., root mean square deviation.

	Native	Ta$_6$Br$_2$	SemetIL21
Data collection			
Beamline	SLS X06DA	SLS X06DA	SLS X06DA
Space group	P2$_1$2$_1$2$_1$	P2$_1$2$_1$2$_1$	P2$_1$2$_1$2$_1$
Cell dimensions	$a = 82.2$, $b = 151.1$, $c = 364.8$ Å;	$a = 82.3$, $b = 151.2$, $c = 364.6$ Å;	$a = 82.0$, $b = 151.0$, $c = 365.6$ Å;
	$\alpha = 90.0°$, $\beta = 90.0°$, $\gamma = 90.0°$	$\alpha = 90.0°$, $\beta = 90.0°$, $\gamma = 90.0°$	$\alpha = 90.0°$, $\beta = 90.0°$, $\gamma = 90.0°$
Resolution (Å)	94.7-2.8 (2.9-2.8)	72.2-6 (8-6)	50-8 (10-8)
R_{merge}	18.7 (71.9)	2.75 (3.8)	3.6 (4.4)
$I/\sigma I$	30.1 (2.08)	52.1 (32.0)	50.0 (43.5)
Completeness (%)	99.7 (82.2)	99.0 (97.6)	97.6 (97.6)
Redundancy	5.2 (4.4)	16.0 (15.8)	13.9 (15.8)
Initial FOM		0.46	
FOM after density modification		0.69	
Refinement			
Resolution (Å)	80.2-2.8		
No. reflections	112,598		
R_{work}/R_{free}	0.25/0.27 (0.37/0.38)		
No. atoms	21,835		
Protein	20,916		
Sugar	711		
Ligand/ion	204		
B-factors			
Wilson *B*-factor	53.7		
Overall *B*-factor	69.5		
Protein	68.0		
Sugar	101.1		
Ligand/ion	105.6		
r.m.s.d.			
Bond lengths (Å)	0.018		
Bond angles	1.352°		

of the eight IL-21R·IL-21 complexes are highly similar. The main difference observed is in the flexible loop connecting helices C and D in IL-21. The interaction surface between IL-21R and IL-21 is identical, however, in the eight structures. The following description represents molecules A (IL-21R) and B (IL-21) in the Protein Data Bank file (code 3TGX).

IL-21R·IL-21 Structure—IL-21R contains two fibronectin III domains that form a V-shaped structure, with the binding site

for the cytokine positioned at the tip of the V (Fig. 1*B*). The two fibronectin domains are connected by a short linker and bent at an angel of ~90°. The D1 domain contains three disulfide bridges: one connecting the N terminus to β-strand 7 (Cys[1]– Cys[90]), one connecting β-strands 1 and 2 (Cys[6]–Cys[16]), and one connecting β-strands 4 and 5 (Cys[46]–Cys[62]). The membrane-proximal domain (D2) does not contain any disulfides but includes a WS*X*WS motif in the F'G' loop, which is character-

istic for class I cytokine receptors. IL-21 exhibits the typical type I cytokine structure composed of a four-helix bundle with an up-up-down-down topology. The finished structure consists of residues 1–208 of IL-21R and residues 2–81 and 89–123 of IL-21, with small variations in the number of built residues between the eight NCS-related molecules. The missing part of IL-21 is the loop connecting helices C and D. This part of the loop is close to neither the IL-21R-binding site nor the predicted γC-binding site.

IL-21R·IL-21 Interface—The interaction between IL-21 and IL-21R is mediated by residues present in helices A and C and by a small part of the CD loop immediately following helix C of IL-21 (Fig. 1, *A* and *B*, and supplemental Table S1). The total binding surface contributed by both IL-21 and IL-21R is 990 Å^2 (calculated using PDBe PISA (40)) and includes extensive sets of polar and apolar interactions (supplemental Table S1). Ten different residues of IL-21 participate in polar interactions with 11 residues of IL-21R. There are 14 residues of IL-21 forming van der Waals contacts with 16 residues of IL-21R. In IL-21, Arg[5], Arg[9], and Gln[12] of helix A and Arg[76] and Lys[73] of helix C are the major contributors to the binding surface. All five residues form extensive polar and van der Waals interactions with residues of IL-21R (supplemental Table S1). Arg[9], Gln[12], Arg[76], and Lys[73] along with Ile[16] form a pocket for Met[70] of IL-21R, the main contributor to the binding surface in IL-21. It is interesting to note that the large hydrophobic side chain of Met[70] fits into a pocket of mainly hydrophilic residues. Met[70] seems to play a crucial role in positioning Arg[9], Gln[12], Arg[76], and Lys[73] correctly in relation to their other interaction partners. Thus, Met[70] positions Arg[9] and Arg[76] of IL-21 for interaction with Asp[72] and Asp[73] of IL-21R, respectively (Fig. 2, *A* and *B*). The IL-21-binding residues of IL-21R are located in the loops connecting the β-strands. The AB, CD, EF, B'C', and F'G' loops and the linker all contain residues involved in binding. In IL-21R, Tyr[36] in the CD loop, Met[70] and Asp[72] in the EF loop, and Tyr[129] in the B'C' loop contribute the most to the binding surface. The most important loop is the EF loop, which supplies 7 of the 20 amino acids of IL-21R that are involved in binding IL-21 (Fig. 1C and supplemental Table S1).

Comparison of Free and Receptor-bound IL-21—The structure of free IL-21 has been previously solved by NMR (34). In contrast to IL-21R-bound IL-21, the structure of the free form contains the N- and C-terminal parts, as well as the CD loop. These are highly disordered, however, explaining why they are absent in the IL-21R·IL-21 structure determined by crystallography. This difference is thus a result of the differences between the techniques of NMR and x-ray crystallography rather than a consequence of ligand binding. In solution, IL-21 exists in equilibrium between two distinct structures, in which helix C is either partially unfolded or formed. The crystal structure reported here indicates that helix C of IL-21 is stabilized upon binding to the receptor. The root mean square deviation using 106 backbone Cα atoms of IL-21 is 1.6 Å (calculated using SSM superimpose in Coot (41)), with the main differences seen in the first part of the CD loop and in the beginning of helix A. In the receptor-bound structure, the N-terminal part of helix A is slightly elongated compared with the free form. This is likely a result of receptor binding, as Arg[5] of IL-21 is present in this
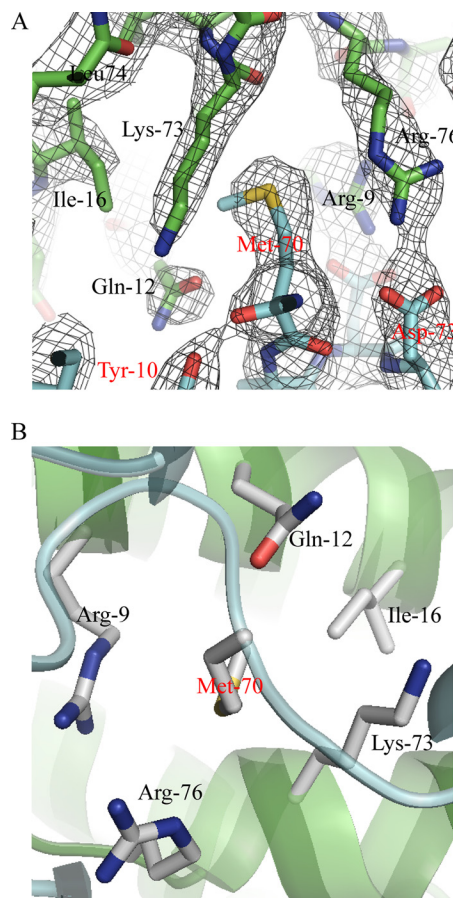

FIGURE 2. **IL-21-binding pocket for Met[70] of IL-21R.** *A*, $2F_o - F_c$ electron density map showing part of the binding interface between IL-21 and IL-21R centered at Met[70] (color code as described for Fig. 1). *B*, binding pocket in IL-21 for Met[70] of IL-21R viewed from IL-21R.

region and interacts with IL-21R (supplemental Table S1). The most noticeable effect of IL-21R binding is observed in the first part of the CD loop of IL-21 (Fig. 3). The CD loop is positioned toward the receptor, allowing Lys[77], Pro[79], and Ser[80] to form a binding pocket for Tyr[36] of the receptor. Previously, a homology model of the IL-21R γC·IL-21 complex was built using the NMR model of IL-21 and the structures of IL-2 in complex with IL-2RA, IL-2RB, and γC, as well as IL-4 in complex with IL-4RA and γC (34). The position of the IL-21R chain predicted in this work is in good agreement with the IL-21R·IL-21 crystal structure presented here.

Sugar Chain Attached to Asn[54] Is Essential for Proper Expression of ECD of IL-21R—The ECD of IL-21R contains five potential N-linked glycosylation sites (Asn[54], Asn[78], Asn[85], Asn[106], and Asn[116]), and the purified ECD of IL-21R recombinantly expressed in HEK293 cells includes ~10-kDa glycans. To establish which sites might be required for receptor integrity, all potential Asn-linked glycosylation sites were individually mutated to Gln, and the effect was evaluated by expression in HEK293 cells. Only the Asn[54]-to-Gln mutation had a profound effect, as it led to an almost complete loss of secreted protein (Fig. 4A). To avoid interference from nonessential sugar residues in both crystallization and biochemical tests, the glycan-minimized ECD of IL-21R (N78Q, N85Q, N106D, and N116Q)
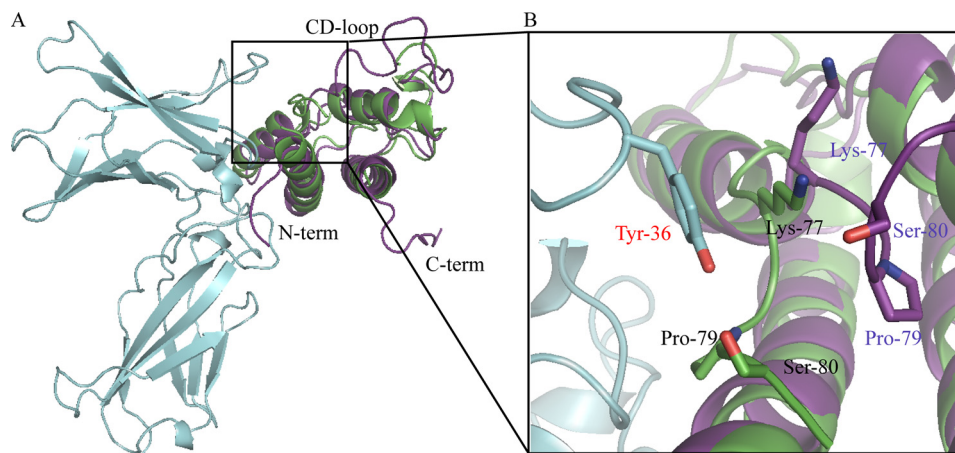
FIGURE 3. **Comparison of IL-21 in solution and IL-21 bound to IL-21R.** The structure of IL-21 in free form solved by NMR (Protein Data Bank code 2OQP; *purple*) was superimposed onto the IL-21R·IL-21 crystal structure (color code as described for in Fig. 1) using SSM superimpose in Coot. The cutout shows an enlargement of the first part of the CD loop of IL-21. Residues of IL-21 forming a pocket for Tyr[36] of the receptor are labeled and color-coded as described for the respective structures.
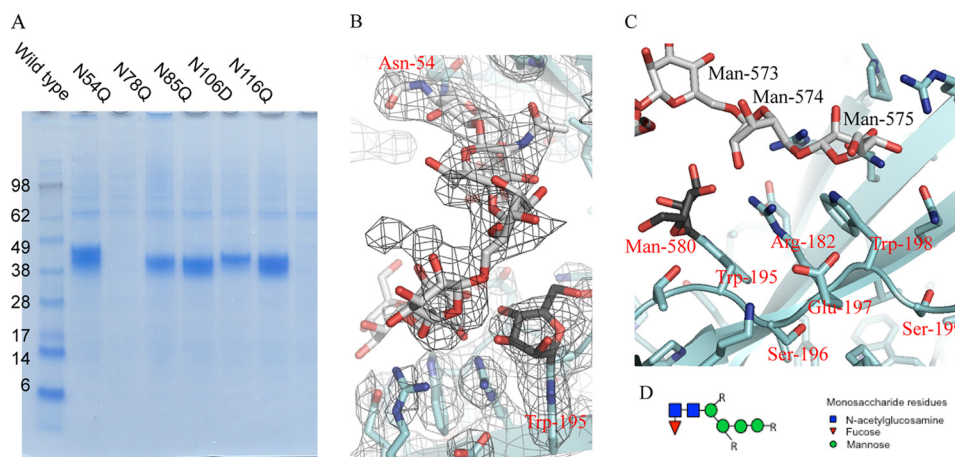

FIGURE 4. **Carbohydrate chain attached to Asn[54] anchors at class I cytokine receptor signature motif (WS*X*WS).** *A*, expression followed by His-tagged purification of the ECD of IL-21R, the wild type, or variants with mutations of the five predicted *N*-linked glycosylation sites as indicated. *B*, $2F_o - F_c$ electron density map (at 1.5σ) around the sugar chain in IL-21R. The color code is as described for Fig. 1. *C*, mannosylated Trp[195] and Arg[182] form multiple hydrogen bonds with the carbohydrate chain originating at Asn[54]. Arg[182] is sandwiched between the two tryptophans of the WS*X*WS motif, forming the W-R-W zipper described in the text. *D*, the glycan structure is heterogeneous. *R* indicates that extra sugar residues might exist at this position, which cannot be built in the electron density. The core structure depicted here is found in the large majority of the glycans. The full glycan structure was determined by mass spectrometry (supplemental Table S2).

was expressed in HEK293 cells. This was the protein used for crystallization.

Two Domains of IL-21R Are Bridged by Sugar Chain That Could Potentially Stabilize Receptor—To our surprise, we found that Asn[54] is connected to the highly conserved WS*X*WS motif by an *N*-linked glycan bridge, which forms a cross-bar, turning the flexible V-shape, formed by the two fibronectin domains, into a seemingly rigidified A-frame (Figs. 1*A* and 4, *B* and *C*). Digestion with peptide:*N*-glucosidase F to deglycosylate the protein failed (data not shown), suggesting that the sugar-based cross-link is an integral part of IL-21R and therefore might be protected from digestion. The composition of the sugar chain attached to Asn[54] was investigated by LC-MS, revealing that the glycosylation is rather heterogeneous (supplemental Table S2). However, a common core consisting of two *N*-acetylglucosamines and four hexoses, most likely mannose, was observed (Fig. 4*D* and supplemental Table S2). In most of the sugar chains, a fucose is also present. The IL-21R

structure presented here has been built to represent this most prevalent glycan chain, *i.e.* with two *N*-acetylglucosamines, four mannoses, and one fucose residue (Figs. 1*A* and 4*B*). The electron density and the LC-MS analysis indicate that additional sugar residues are present in the receptor chain (Fig. 4, *B* and *D*, and supplemental Table S2). However, these cannot be placed with confidence due to the heterogeneity of the glycosylation and the possible flexibility of the sugars, which do not engage in the hydrogen bonding network described above. The position of the additional glycosylation is indicated in Fig. 4*D*.

Mannosylation at First Tryptophan in WSXWS Motif Forms Extensive Hydrogen Bonding Network with Sugar Chain Originating from Asn[54]—The hydrogen bonding network between the sugar chain and the WS*X*WS motif offers a unique insight into how glycans can be integrated into protein structures (Fig. 4*C* and Table 2). Arg[182] is held tightly in place between the two Trp residues, with its charged headgroup exposed, allowing it to form hydrogen bonds with the sugar chain. Furthermore, an

TABLE 2
Hydrogen bonds connecting the Asn[54] *N*-linked sugar to the second fibronectin domain of IL-21R and Trp[195]-linked Man[580]

N-Linked sugar/atom	IL-21R or Man[580]	Atom	Distance
			Å
Man[574]			
O2	Man[580]	O4	2.4
O2	Man[580]	O2	2.1
O2	Arg[186]	NH1	3.3
O2	Arg[154]	NH1	3.5
O2	Arg[186]	N2	3.2
O3	Man[580]	O4	2.9
O5	Arg[154]	NH2	3.3
O6	Trp[198]	NE1	3.4
Man[575]			
O3	Gln[140]	OE1	2.8
O3	Gln[140]	NE2	2.7
O3	Arg[142]	NH2	3.5
O4	Gln[180]	OE1	3.3
O5	Trp[198]	NE1	2.9

additional density was observed around Trp[195], suggesting that this residue was modified. Indeed, protease digestion followed by LC-MS analysis confirmed that Trp[195] is *C*-mannosylated at C1 of the indole ring (data not shown). Thus, the carbohydrate chain originating from Asn[54] forms multiple hydrogen bonds not only with Arg[182] but also with mannosylated Trp[195] (Fig. 4*C* and Table 2).

DISCUSSION

The complex between IL-21R and IL-21 bears considerable resemblance to the other γC-binding cytokines complexed with their corresponding receptors. The binding interactions are mediated by residues present in the loops of both of the fibronectin domains of the receptor contacting residues of helices A and C and the first part of the CD loop of IL-21. The overall structure of IL-21 bound to IL-21R is quite similar to the structure of IL-21 in solution, with the most prominent difference being a rearrangement of the first part of the CD loop, leading to formation of a pocket providing binding of Tyr[36] of the receptor. Free IL-21 exists in two distinct forms in solution; one has a structured helix C and the other an unstructured region within this segment. The IL-21R·IL-21 crystal structure demonstrates that it is the IL-21 conformation that has a structured helix C that is bound by the receptor. In line with this, it was previously determined that stabilization of helix C and the first part of the CD loop of IL-21 by replacing them with the equivalent part of IL-4 leads to a ligand of significantly higher activity (34). Helix C in IL-4 is more ordered than its counterpart in IL-21. The increase in ligand potency was thus proposed to arise as a result of chimeric IL-21 presenting helix C and the CD loop more favorable for functional interaction with IL-21R.

Our structure is the first type II cytokine structure to display partial mammalian glycosylation. We observed that the highly conserved WS*X*WS motif is *C*-mannosylated at the first Trp, as would be expected from prior biochemical work (31–33, 42). Thus, for the first time, we can visualize the structural consequences of this modification. Interestingly, the structure furthermore reveals that Asn[54] of the D1 domain of IL-21R is connected to the WS*X*WS motif in the D2 domain by an *N*-linked glycan bridge. The sugar chains are in solvent channels in the crystal and are thus not close to any crystal contacts. The posi-

tion of the sugar is thus not an artifact of the crystal packing. We have shown that the sugar chain attached to Asn[54] is required for proper cell surface expression of IL-21R, whereas the remaining sugars are not. We consider it unlikely that the general folding of the receptor is impaired by the absence of Asn[54] glycosylation. In the previously published structures of class I cytokine receptor complexes, the ECDs of the receptors were produced in insect cells, which do not yield the same type of glycosylation as mammalian cells (19, 21, 29, 43, 44). As these structures were solved without the carbohydrate bridge, it cannot be essential for the folding of individual domains. Previous studies have shown, however, that even minimal glycosylation of IL-7R enhances the affinity for IL-7 (20). Whether this is also the case for other members of the family remains to be determined. Biochemical studies of EPOR have shown that mutations within the WS*X*WS motif impair export of EPOR to the cell surface and lead to accumulation in the Golgi (25, 45). In particular, the first Trp of the WS*X*WS showed no tolerance for substitution. Interestingly, EPOR has an N-terminal helix that takes up the space between the D1 and D2 domains, making contact with the WS*X*WS motif (23). This helix thus occupies the same position as the glycan bridge in IL-21R. It is tempting to speculate that the sugar bridge has an influence on IL-21R signaling, possible via a stabilizing effect on the ECD of IL-21R. However, we have been unable to address this important question properly, as mutations that eliminate the sugar chain originating from Asn[54] also impair cell surface expression of the receptor.

Several members of the class I cytokine receptor family have potential *N*-linked glycosylation sites in the D1 domain facing the D2 domain (*e.g.* IL-2RB has Asn[17], γC has Asn[49], and IL-7R has Asn[29]) (17, 20). Most of the previous structures of type I cytokine complexes use receptors expressed in insect cells, which show less complex glycosylation patterns than mammalian cells and do not mannosylate the WS*X*WS sequence (19, 21, 29, 43). These structures can thus not help elucidate whether the *N*-linked glycan bridge observed in the IL-21R structure, is a specific feature of IL-21R or a more general feature of the class I cytokine receptor family.

REFERENCES

1. Kang, L., Bondensgaard, K., Li, T., Hartmann, R., and Hjorth, S. A. (2010) Rational design of interleukin-21 antagonist through selective elimination of the γC binding epitope. *J. Biol. Chem.* **285,** 12223–12231
2. Spolski, R., and Leonard, W. J. (2010) IL-21 and T follicular helper cells. *Int. Immunol.* **22,** 7–12
3. Johnston, R. J., Poholek, A. C., DiToro, D., Yusuf, I., Eto, D., Barnett, B., Dent, A. L., Craft, J., and Crotty, S. (2009) Bcl6 and Blimp-1 are reciprocal and antagonistic regulators of T follicular helper cell differentiation. *Science* **325,** 1006–1010
4. Korn, T., Bettelli, E., Gao, W., Awasthi, A., Jäger, A., Strom, T. B., Oukka, M., and Kuchroo, V. K. (2007) IL-21 initiates an alternative pathway to induce proinflammatory T$_H$17 cells. *Nature* **448,** 484–487
5. Nurieva, R., Yang, X. O., Martinez, G., Zhang, Y., Panopoulos, A. D., Ma, L., Schluns, K., Tian, Q., Watowich, S. S., Jetten, A. M., and Dong, C. (2007)

Essential autocrine regulation by IL-21 in the generation of inflammatory T cells. *Nature* **448,** 480–483

6. Nurieva, R. I., Chung, Y., Hwang, D., Yang, X. O., Kang, H. S., Ma, L., Wang, Y. H., Watowich, S. S., Jetten, A. M., Tian, Q., and Dong, C. (2008) Generation of T follicular helper cells is mediated by interleukin-21 but independent of T helper 1, 2, or 17 cell lineages. *Immunity* **29,** 138–149

7. Vogelzang, A., McGuire, H. M., Yu, D., Sprent, J., Mackay, C. R., and King, C. (2008) A fundamental role for interleukin-21 in the generation of T follicular helper cells. *Immunity* **29,** 127–137

8. Nurieva, R. I., Chung, Y., Martinez, G. J., Yang, X. O., Tanaka, S., Matskevitch, T. D., Wang, Y. H., and Dong, C. (2009) Bcl6 mediates the development of T follicular helper cells. *Science* **325,** 1001–1005

9. Zeng, R., Spolski, R., Finkelstein, S. E., Oh, S., Kovanen, P. E., Hinrichs, C. S., Pise-Masison, C. A., Radonovich, M. F., Brady, J. N., Restifo, N. P., Berzofsky, J. A., and Leonard, W. J. (2005) Synergy of IL-21 and IL-15 in regulating CD8$^+$ T cell expansion and function. *J. Exp. Med.* **201,** 139–148

10. Ozaki, K., Spolski, R., Feng, C. G., Qi, C. F., Cheng, J., Sher, A., Morse, H. C., 3rd, Liu, C., Schwartzberg, P. L., and Leonard, W. J. (2002) A critical role for IL-21 in regulating immunoglobulin production. *Science* **298,** 1630–1634

11. Elsaesser, H., Sauer, K., and Brooks, D. G. (2009) IL-21 is required to control chronic viral infection. *Science* **324,** 1569–1572

12. Fröhlich, A., Kisielow, J., Schmitz, I., Freigang, S., Shamshiev, A. T., Weber, J., Marsland, B. J., Oxenius, A., and Kopf, M. (2009) IL-21R on T cells is critical for sustained functionality and control of chronic viral infection. *Science* **324,** 1576–1580

13. Yi, J. S., Du, M., and Zajac, A. J. (2009) A vital role for interleukin-21 in the control of a chronic viral infection. *Science* **324,** 1572–1576

14. Hashmi, M. H., and Van Veldhuizen, P. J. (2010) Interleukin-21: updated review of Phase I and II clinical trials in metastatic renal cell carcinoma, metastatic melanoma, and relapsed/refractory indolent non-Hodgkin lymphoma. *Expert Opin. Biol. Ther.* **10,** 807–817

15. Rochman, Y., Spolski, R., and Leonard, W. J. (2009) New insights into the regulation of T cells by γC family cytokines. *Nat. Rev. Immunol.* **9,** 480–490

16. Asao, H., Okuyama, C., Kumaki, S., Ishii, N., Tsuchiya, S., Foster, D., and Sugamura, K. (2001) Cutting edge: the common γ-chain is an indispensable subunit of the IL-21 receptor complex. *J. Immunol.* **167,** 1–5

17. Zhang, J. L., Foster, D., and Sebald, W. (2003) Human IL-21 and IL-4 bind to partially overlapping epitopes of common γ-chain. *Biochem. Biophys. Res. Commun.* **300,** 291–296

18. Bravo, J., Staunton, D., Heath, J. K., and Jones, E. Y. (1998) Crystal structure of a cytokine-binding region of gp130. *EMBO J.* **17,** 1665–1674

19. LaPorte, S. L., Juo, Z. S., Vaclavikova, J., Colf, L. A., Qi, X., Heller, N. M., Keegan, A. D., and Garcia, K. C. (2008) Molecular and structural basis of cytokine receptor pleiotropy in the interleukin-4/13 system. *Cell* **132,** 259–272

20. McElroy, C. A., Dohm, J. A., and Walsh, S. T. (2009) Structural and biophysical studies of the human IL-7/IL-7Rα complex. *Structure* **17,** 54–65

21. Wang, X., Rickert, M., and Garcia, K. C. (2005) Structure of the quaternary complex of interleukin-2 with its α, β, and γC receptors. *Science* **310,** 1159–1163

22. Hage, T., Sebald, W., and Reinemer, P. (1999) Crystal structure of the interleukin-4/receptor α-chain complex reveals a mosaic binding interface. *Cell* **97,** 271–281

23. Livnah, O., Stura, E. A., Middleton, S. A., Johnson, D. L., Jolliffe, L. K., and Wilson, I. A. (1999) Crystallographic evidence for preformed dimers of erythropoietin receptor before ligand activation. *Science* **283,** 987–990

24. Tauber, M. T., Porra, V., Dastot, F., Molinas, C., Amselem, S., Cholin, S., Rochiccioli, P., and Bieth, E. (1998) Heterozygous mutation in the WS*X*WS equivalent motif of the growth hormone receptor in a child with poor response to growth hormone therapy. *Growth Horm. IGF Res.* **8,** 211–216

25. Hilton, D. J., Watowich, S. S., Katz, L., and Lodish, H. F. (1996) Saturation mutagenesis of the WS*X*WS motif of the erythropoietin receptor. *J. Biol. Chem.* **271,** 4699–4708

26. Chiba, T., Amanuma, H., and Todokoro, K. (1992) Tryptophan residue of Trp-Ser-*X*-Trp-Ser motif in extracellular domains of erythropoietin receptor is essential for signal transduction. *Biochem. Biophys. Res. Commun.* **184,** 485–490

27. Miyazaki, T., Maruyama, M., Yamada, G., Hatakeyama, M., and Taniguchi, T. (1991) The integrity of the conserved "WS motif" common to IL-2 and other cytokine receptors is essential for ligand binding and signal transduction. *EMBO J.* **10,** 3191–3197

28. Quelle, D. E., Quelle, F. W., and Wojchowski, D. M. (1992) Mutations in the WSAWSE and cytosolic domains of the erythropoietin receptor affect signal transduction and ligand binding and internalization. *Mol. Cell. Biol.* **12,** 4553–4561

29. Hansen, G., Hercus, T. R., McClure, B. J., Stomski, F. C., Dottore, M., Powell, J., Ramshaw, H., Woodcock, J. M., Xu, Y., Guthridge, M., McKinstry, W. J., Lopez, A. F., and Parker, M. W. (2008) The structure of the GM-CSF receptor complex reveals a distinct mode of cytokine receptor activation. *Cell* **134,** 496–507

30. Baumgartner, J. W., Wells, C. A., Chen, C. M., and Waters, M. J. (1994) The role of the WS*X*WS equivalent motif in growth hormone receptor function. *J. Biol. Chem.* **269,** 29094–29101

31. Furmanek, A., and Hofsteenge, J. (2000) Protein *C*-mannosylation: facts and questions. *Acta Biochim. Pol.* **47,** 781–789

32. Doucey, M. A., Hess, D., Blommers, M. J., and Hofsteenge, J. (1999) Recombinant human interleukin-12 is the second example of a *C*-mannosylated protein. *Glycobiology* **9,** 435–441

33. Furmanek, A., Hess, D., Rogniaux, H., and Hofsteenge, J. (2003) The WSAWS motif is *C*-hexosylated in a soluble form of the erythropoietin receptor. *Biochemistry* **42,** 8452–8458

34. Bondensgaard, K., Breinholt, J., Madsen, D., Omkvist, D. H., Kang, L., Worsaae, A., Becker, P., Schiødt, C. B., and Hjorth, S. A. (2007) The existence of multiple conformers of interleukin-21 directs engineering of a superpotent analogue. *J. Biol. Chem.* **282,** 23326–23336

35. Kabsch, W. (2010) Integration, scaling, space-group assignment and post-refinement. *Acta Crystallogr. D Biol. Crystallogr.* **66,** 133–144

36. Sheldrick, G. M. (2010) Experimental phasing with SHELXC/D/E: combining chain tracing with density modification. *Acta Crystallogr. D Biol. Crystallogr.* **66,** 479–485

37. Adams, P. D., Afonine, P. V., Bunkóczi, G., Chen, V. B., Davis, I. W., Echols, N., Headd, J. J., Hung, L. W., Kapral, G. J., Grosse-Kunstleve, R. W., McCoy, A. J., Moriarty, N. W., Oeffner, R., Read, R. J., Richardson, D. C., Richardson, J. S., Terwilliger, T. C., and Zwart, P. H. (2010) Phenix: a comprehensive Python-based system for macromolecular structure solution. *Acta Crystallogr. D Biol. Crystallogr.* **66,** 213–221

38. Terwilliger, T. C. (2003) Improving macromolecular atomic models at moderate resolution by automated iterative model building, statistical density modification, and refinement. *Acta Crystallogr. D Biol. Crystallogr.* **59,** 1174–1182

39. Emsley, P., Lohkamp, B., Scott, W. G., and Cowtan, K. (2010) Features and development of Coot. *Acta Crystallogr. D Biol. Crystallogr.* **66,** 486–501

40. Velankar, S., and Kleywegt, G. J. (2011) The Protein Data Bank in Europe (PDBe): bringing structure to biology. *Acta Crystallogr. D Biol. Crystallogr.* **67,** 324–330

41. Emsley, P., and Cowtan, K. (2004) Coot: model-building tools for molecular graphics. *Acta Crystallogr. D Biol. Crystallogr.* **60,** 2126–2132

42. Hofsteenge, J., Müller, D. R., de Beer, T., Löffler, A., Richter, W. J., and Vliegenthart, J. F. (1994) New type of linkage between a carbohydrate and a protein: *C*-glycosylation of a specific tryptophan residue in human RNase Us. *Biochemistry* **33,** 13524–13530

43. Chow, D., He, X., Snow, A. L., Rose-John, S., and Garcia, K. C. (2001) Structure of an extracellular gp130 cytokine receptor signaling complex. *Science* **291,** 2150–2155

44. Stauber, D. J., Debler, E. W., Horton, P. A., Smith, K. A., and Wilson, I. A. (2006) Crystal structure of the IL-2 signaling complex: paradigm for a heterotrimeric cytokine receptor. *Proc. Natl. Acad. Sci. U.S.A.* **103,** 2788–2793

45. Hilton, D. J., Watowich, S. S., Murray, P. J., and Lodish, H. F. (1995) Increased cell surface expression and enhanced folding in the endoplasmic reticulum of a mutant erythropoietin receptor. *Proc. Natl. Acad. Sci. U.S.A.* **92,** 190–194